Journal of Computational Applied Mechanics 2021, 52(3): 408-422
DOI: 10.22059/jcamech.2021.322563.613

RESEARCH PAPER

A comparative study of crack detection in nanobeams using molecular dynamics, analytical and finite element methods

Seyyed Sajad Mousavi Nejad Souq[1], Faramarz Ashenai Ghasemi[1,*], Mir Masoud Seyyed Fakhrabadi[2]

[1] Faculty of Mechanical Engineering, Shahid Rajaee Teacher Training University, Tehran, Iran

[2] School of Mechanical Engineering, College of Engineering, University of Tehran, Tehran, Iran

Abstract

The study of material behavior in the presence of defects is one of the studies that can help us recognize and predict material behavior. Studying the behavior of materials in nanoscale illuminates a broad view of the behavior of materials. A variety of studies are available for such a study: numerical, experimental, and quasi-experimental methods. Molecular dynamics is one of the methods that can be used to study the behavior of materials. The vibrational behavior of structures has been the focus of many researchers to analyze and investigate mortar materials' properties. The study of vibrational behavior at the nanoscale can give us a broad view of materials' properties. Therefore, in this study, we study nanowires' vibrational behavior in the presence of edge cracks using molecular dynamics. The influence of crack position and depth on the natural frequencies and shape of iron nanobeam modes with BCC crystal structure have been investigated. Clamped-Clamped boundary conditions with different cracks position and depth have been applied by simulating molecular dynamics. Also, the data obtained from molecular dynamics simulations have been compared with the finite element method and different crack models in one dimensional beams . In order to extract the shape of natural modes and frequencies by molecular dynamics method, FFT applied on the displacement history of nanobeam atoms after excitation of an amplitude in the center of nanobeam in x and y directions have been used. The crack models studied in this study were linear and rotational crack models on beams with Timoshenko theory. Molecular dynamics simulation data compared to other methods have shown a decrease in the value of natural frequencies in the presence of cracks. Also, finite element data and molecular dynamics are well matched. However, the molecular dynamics method has shown a more significant reduction in natural frequency values than finite element methods and various crack models with Timoshenko theory. We have also found that in molecular dynamics bribery, the initial excitation type of nanobeams is very useful in extracting nanobeam modes' shape.

Keywords: Cracked Nanobeam, Molecular Dynamics Simulation, Vibration Analysis, Finite Element Method.

Introduction

Nano- and micro-electromechanical systems (NEMS/MEMS) are extensively applied in mechanical resonators, chemical and biochemical sensors, and relays in logic devices. Many NEMS such as high-frequency resonators [1,2], pressure and force sensors [2], and nano switches [3] use nanobeams/nanowires as their active elements thanks to the unique mechanical

* Corresponding Author. *Email Address*: f.a.ghasemi@sru.ac.ir

and vibrational properties of nanoscale objects. Hence, the vibrational behavior of nanobeams has been the subject of many experimental, theoretical, and computational research studies [4-8]. On the theoretical and computational side, several works employed molecular dynamics (MD) and continuum mechanics to investigate their mechanical and vibrational properties [8-12]. Several authors used the various analytical or computational approaches to the analysis of non-cracked nanobeam problem and surface properties estimation. [13 -17].

The crack is a commonly observed structural defect that can decrease the stiffness and strength of the structures [18 -21]. Early-stage detection of the cracks is a vital inspection necessity that can lead to hazardous incidents, otherwise. *Since the* natural frequencies of the structures directly relate to their stiffness, they are frequently used to identify the location and depth of the crack. Chondros et al. [22] developed a continuum mechanics-based theory for the lateral vibration of cracked Euler–Bernoulli beams with single-edge or double-edge open cracks. They showed that the natural frequency of the cracked beam decreases as the crack depth increases. Also, some studies got natural frequencies for the detection of crack location and size or investigated the dynamic behavior of cracked beams [23-25]. Baradaran and Mousavi [24], due to the changes in natural frequencies in the presence of cracks compared to beams without cracks, with finite element method and applying the Ants colony optimization algorithm as an inverse problem, obtained the position and depth of surface cracks in the beam. Some studies define a reduced elastic modulus zone in the crack location and model this reduction by a rotational spring [21, 22, 26-32] or combined rotational and translational springs in the given position [30, 33]. *In addition,* many studies analyzed the vibration characteristics of the cracked beams using finite element method (FEM). They obtained the variation of natural frequencies vs. the crack depth and positions [34 -39]. Despite the extensive studies on the effects of cracks on the natural frequencies of macroscale structures, to the best of our knowledge, no research report in the literature analyzed the effects of crack on the vibrational behavior of metallic nanobeams. In this work, we want to shed light on the degrees of the appropriateness of the developed techniques to model such effects at macroscales to be used for nanoscale beams by comparison of the results from MD simulation, FEM, and analytical equations.

Methodology

This section provides detailed information of three techniques used to analyze the crack effects on the natural frequencies of the metallic, here Fe, nanowires. The first sub-section explains the steps of MD simulations to acquire the natural frequencies and mode shapes of the nanobeam. In the second sub-section, the theory of one-dimensional Timoshenko beam and spring models of the cracks are described. In the third sub-section, the details of the three-dimensional FE model of the nanobeam to obtain the mode shapes and frequencies are elaborated.

Molecular dynamic simulation

In the present work, the nanobeam with the length of 28.6 nm and the cross-section of 5.73×2.86 nm^2 is investigated (see Fig. 1). The interactions between the Fe atoms are modeled by the embedded atom method (EAM) potential function of the form:

$$E_i = F_\alpha\left(\sum_{i\neq j}\rho_\beta(r_{ij})\right) + \frac{1}{2}\sum_{i\neq j}\phi_{\alpha\beta}(r_{ij}) \tag{1}$$

where r_{ij} is the distance between atoms i and j, $\phi_{\alpha\beta}$ is a pairwise potential function, ρ_β is the contribution to electron charge density from atom j at the location of atom i and F_α is an

embedding function representing the energy required to place atom i into the electron cloud. Also, α and βare the element types of atom i and j, respectively. The EAM potential developed by Mendelev [31] is used in the MD simulations.

The crack location normalized by nanobeam length is varied from 0.1 to 0.5 in steps of 0.1 and the crack depth normalized by nanobeam thickness is varied from 0.1 to 0.7 in steps of 0.1.

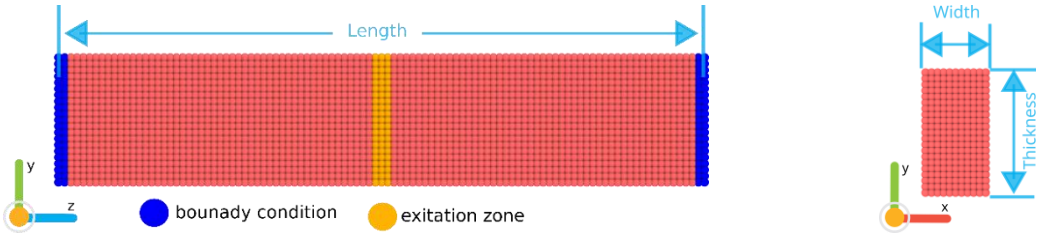

Figure 1. The nanobeam for MD simulations.

In the vibration tests, the nanobeams were minimized by iteratively adjusting atom coordinates based on the conjugate gradient method. After that, the nanobeams are thermally equilibrated using the NVT ensemble for 50 ps. A Nose–Hoover thermostat was employed to keep the temperature constant at 1 K. At this point, the two ends of the beams, i. e. two lattice constant lengths of atoms on each side, are kept rigid to simulate the clamped-clamped boundary condition.

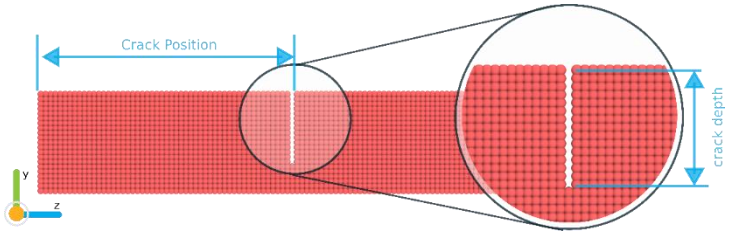

Figure 2. Cracked beam and the properties of induced crack.

When the system was fully equilibrated, the ensemble was switched to NVE. In two separate simulations, we applied a "fix" displacement to move 1.5 Å of the atoms' positions in the "excitation" zone in the x and y directions. To dumping the vibrations of the nanobeams, the samples equilibrated for 5 ns. After 5 ns equilibration, the time history of nanobeams' external atoms position was recorded as a time-domain response within the last 5 ns.

The motion equations were solved using the velocity Verlet algorithm with a timestep of 1 fs for both excitation and vibrational tests to calculate atomic displacements. All the simulations were performed using LAMMPS [32], and visualization was done using Ovito [40].

Extraction of nanobeam mode shapes and frequencies

The mode shapes and resonant frequencies of nanobeams were obtained from processing raw data of the MD simulations using the Fast Fourier Transform (FFT) of atomic displacement history. The resonant frequencies were determined based on the peaks of the frequency response diagrams obtained from the autocorrelation functions in the frequency domain in three directions as:

$$F^i_{x-corr}(\omega) = F^i_x(\omega)\overline{F^i_x(\omega)}$$
$$F^i_{y-corr}(\omega) = F^i_y(\omega)\overline{F^i_y(\omega)} \quad (2)$$
$$F^i_{z-corr}(\omega) = F^i_z(\omega)\overline{F^i_z(\omega)}$$

where ω is the frequency-dependent complex number, $F^i_x(\omega)$, $F^i_y(\omega)$ and $F^i_z(\omega)$ are the outputs of FFT for the coordinates of the i^{th} atom and the bar sign represents the complex conjugate. The frequency responses in the x, y, and z directions were plotted by the summation of these expressions for all atoms. To extract the vibrational mode shapes, the cross-correlations of atoms in the frequency domain (Eq. (3)) were used.

$$F^i_{x-cros}(\omega_{res}) = F^i_x(\omega_{res})\overline{F^{ref}_R(\omega_{res})}$$
$$F^i_{y-cros}(\omega_{res}) = F^i_y(\omega_{res})\overline{F^{ref}_R(\omega_{res})} \quad (3)$$
$$F^i_{z-cros}(\omega_{res}) = F^i_z(\omega_{res})\overline{F^{ref}_R(\omega_{res})}$$

where ω_{res} is the resonant frequency and the subscript R refers to the maximum power component between (x, y, z) at the specified resonant frequency. By selecting a reference atom (ref superscript in Eq. (3)) which must be neither on the node of mode shape nor on the fixed end of the beams, the cross-correlations were calculated. The real part of each term on the left-hand side of cross-correlation relations for each atom was divided by the maximum absolute value of the real parts of the cross-correlations for all atoms. The results of this part were three real numbers, corresponding to three displacements in the x, y, and z directions, for each atom in the range of $[-1,1]$. By multiplication to the normalized numbers and a proper scaling factor, the displacements of all atoms from their initial positions were obtained. Then, adding these displacements to the initial positions, the mode shape of each resonant frequency (ω_{res}) were extracted.

Timoshenko beam theory for cracked beams

For a Timoshenko beam, the strain energy (U) with both bending and shear contributions and the kinetic energy (T) are given by:

$$U = \frac{1}{2}\int_0^L \left[EI(x)\left(\frac{\partial\theta}{\partial x}\right)^2 + \kappa GA\left(\frac{\partial w}{\partial x} - \theta\right)^2\right]dx \quad (4)$$

$$T = \frac{1}{2}\int_0^L \left[\rho A(x)\left(\frac{\partial w}{\partial t}\right)^2 + \rho I\left(\frac{\partial\theta}{\partial t}\right)^2\right]dx \quad (5)$$

where L, I, and A are the length of the beam, the moment of inertia, and the cross-sectional area. Also, E, G, and ρ denote Young's and shear moduli and mass density per unit length. The letter κ is the shape factor of cross-section (for square cross-section is 5/6), and w and θ are the transverse displacement and rotation of the beam. For a linear elastic beam, the bending moment and the shear force are [41]:

$$EI\frac{\partial\theta(x)}{\partial x} = M(x) \quad (6)$$

$$\kappa GA\left(\frac{\partial w(x)}{\partial x} - \theta(x)\right) = Q(x) \quad (7)$$

For a beam with a crack, additional strain energy (π_c) is expressed as [42]:

$$\pi_c = \int_A J\, dA \tag{8}$$

where J is the function of strain energy release rate depending on stress intensity factors for cracks as:

$$J = \frac{1}{E'}\left[K_{IM}^2 + K_{IIQ}^2\right] \tag{9}$$

where $E' = \frac{E}{1-\upsilon^2}$ for the plane strain and $E' = E$ for the plane stress, υ is the Poisson's ratio, and K_I and K_{II} are the stress intensity factors in fracture modes I and II, respectively. Then,

$$K_{IM} = \sigma F_I\left(\frac{a}{h}\right)\sqrt{\pi a}, \qquad \sigma = \frac{6M}{bh^2} \tag{10}$$

$$K_{IIQ} = \tau F_{II}\left(\frac{a}{h}\right)\sqrt{\pi a}, \qquad \tau = \frac{\kappa Q}{bh} \tag{11}$$

where F_I and F_{II} are the correction factors of stress intensity factors and a is the crack depth. Based on the Paris equation, the additional defection caused by the crack in the direction of P_i is:

$$w_i = \frac{\partial \pi_c(P_i, A)}{\partial P_i} = \frac{\partial}{\partial P_i}\int_A J(P_i, A)\, dA \tag{12}$$

The flexibility coefficients can be expressed as [38]:

$$c_{ij} = \frac{\partial w_i}{\partial P_i} = \frac{\partial^2 \pi_c}{\partial P_i P_j} \tag{13}$$

where P_i and P_j donate the sharing force Q and bending moment M, respectively. Based on Eqs. (9), (10) and (12), the flexibility coefficients are:

$$c_{11} = \frac{2\pi}{Eb^2h^2}\kappa^2 \int_{-b}^{b}\int_0^a \zeta F_{II}^2\left(\frac{\zeta}{h}\right) d\zeta\, dz \tag{14}$$

$$c_{22} = \frac{72\pi}{Eb^2h^4}\int_{-b}^{b}\int_0^a \zeta F_I^2\left(\frac{\zeta}{h}\right) d\zeta\, dz \tag{15}$$

where c_{11} is the flexibility coefficient corresponding to fracture mode II due to shearing force and c_{22} is the flexibility coefficient corresponding to fracture mode I due to bending moment. In the cracked section of the beam, the spring stiffness coefficients are:

$$K_{wc} = \frac{1}{c_{11}} \tag{16}$$

$$K_{\theta c} = \frac{1}{c_{22}} \tag{17}$$

where $K_{\omega c}$ and $K_{\theta c}$ are the translational and rotational spring stiffnesses, respectively. Each model in this paper is named by the selected correction factors.

The Crack models

Here, three models for rotational springs and one model for translational spring are introduced. The first model has two separated rotational and translational springs. For this model, we used the correction factors reported by Tada and Hiroshi [42] for all crack depth ($0 < \left(\frac{\zeta}{h}\right) < 1$):

$$F_I\left(\frac{\zeta}{h}\right)=\sqrt{\frac{2h}{\pi\zeta}\tan\left(\frac{\pi\zeta}{2h}\right)}\frac{0.923+0.199\left(1-\sin\left(\frac{\pi\zeta}{2h}\right)^2\right)}{\cos\left(\frac{\pi\zeta}{2h}\right)} \tag{18}$$

$$F_{II}\left(\frac{\zeta}{h}\right)=\frac{1.122-0.561\left(\frac{\zeta}{h}\right)+0.085\left(\frac{\zeta}{h}\right)^2+0.180\left(\frac{\zeta}{h}\right)^3}{\sqrt{1-\left(\frac{\zeta}{h}\right)}} \tag{19}$$

This research's second model is a rotational spring model of the brown correction factor, and a translational spring donates to Eq 19. The rotational spring model of the brown was developed for a crack depth range of $0<\left(\frac{\zeta}{h}\right)<0.7$ [42]:

$$F_I\left(\frac{\zeta}{h}\right)=1.122-1.40\left(\frac{\zeta}{h}\right)+7.33\left(\frac{\zeta}{h}\right)^2-13.08\left(\frac{\zeta}{h}\right)^3+14.0\left(\frac{\zeta}{h}\right)^4 \tag{20}$$

The third crack model used in this study is a rotational spring model presented by Lellep [43] for a depth range of $0<\left(\frac{\zeta}{h}\right)<0.7$:

$$F_I\left(\frac{\zeta}{h}\right)=1.93-3.07\left(\frac{\zeta}{h}\right)+14.53\left(\frac{\zeta}{h}\right)^2-25.11\left(\frac{\zeta}{h}\right)^3+25.8\left(\frac{\zeta}{h}\right)^4 \tag{21}$$

Fig. 3. presents the shape of Eqs. (18) -(21). There is a difference between Eq. (21) and other equations in the start position. But it is seen that Eqs. (18) and (21) have the same trend. With increasing the crack depth, the differences increase, as well causing different behaviors of models for deeper cracks.

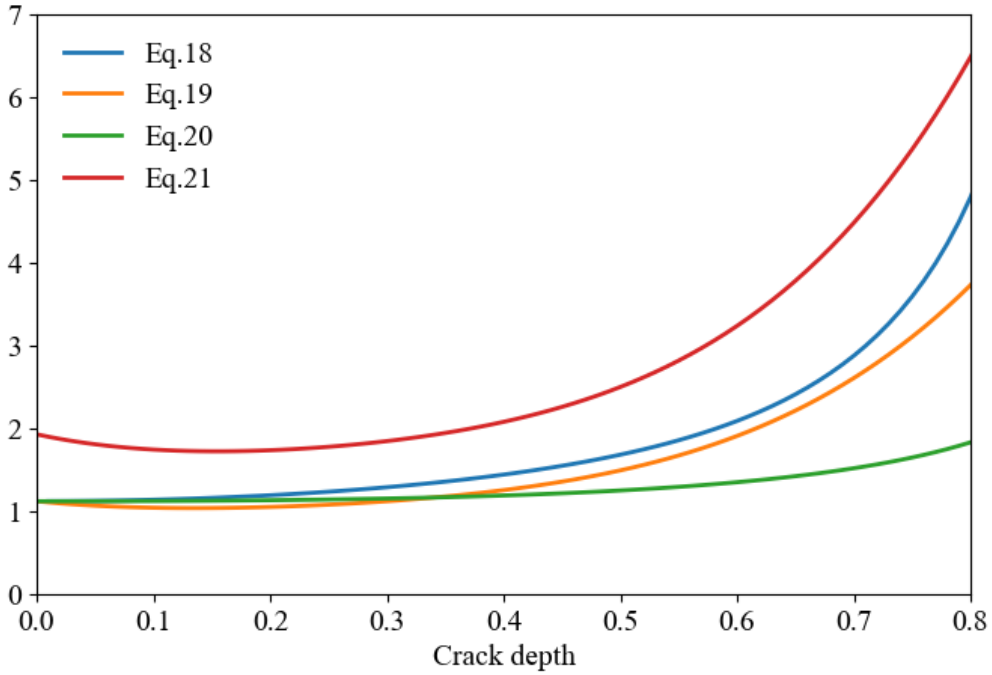

Figure 3. Comparison of the correction factors vs. the crack depth.

Finite element model

To extract natural frequencies and their corresponding mode shapes of the 3D beam model with cracks, we employed the FE software COMSOL multiphysics version 5.4 [44]. The Eigen frequency study in the solid mechanic's interface was used to compute Eigen modes

(vibrational mode shapes) and Eigen frequencies (vibrational frequencies) of the linear model. COMSOL Multiphysics utilizes four different element types: tetrahedral (tets), hexahedral (bricks), triangular prisms (prisms), and pyramids. In this study, all models were meshed by the tetrahedral element type. The size and elastic properties of the beam in COMSOL were considered based on the data from MD simulations. The Young's modulus, Poisson ratio, and Density were selected 221×10^9 GPa, 0.3, and 7800 Kg/m3, respectively.

Results and discussion

In this section, we present data extracted from the MD, FEM, and theoretical crack models. First, the mode shapes are presented from the FE software, and then these shapes are compared with the data obtained from MD simulation. Afterward, the data from analytical crack models are compared with the MD and FEM results.

Finite element method

Nine vibrational mode shapes from FEM are observed in Fig. 4. The first, fourth, and sixth mode shapes are in the XZ-plane of the beam, the second, fifth, eighth, and ninth modes are in the YZ-plane, and others combinational.

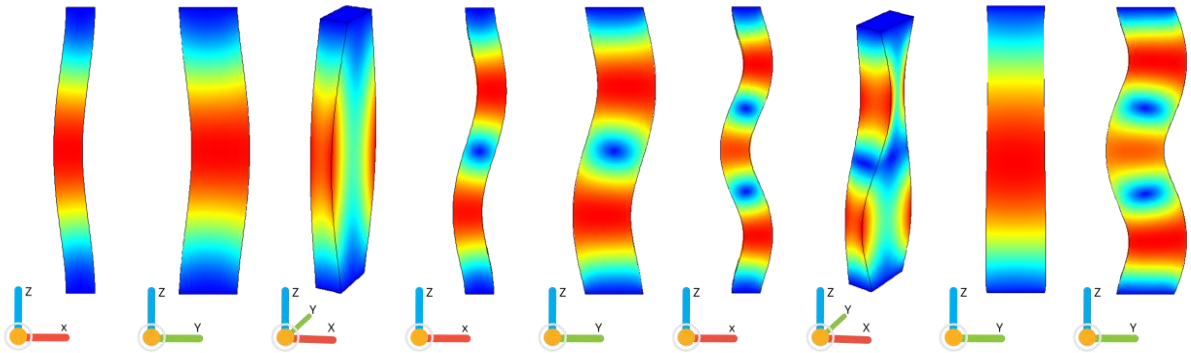

Figure 4. Nine vibrational mode shapes of a nanobeam from COMSOL Multiphysics.

Investigation of the mode shapes from MD simulations and their corresponding frequencies reveals that the three mode shapes shown in Fig. 5 are identical. The value of natural frequencies from MD and FEM in the non-cracked beam agree with each other (Table. 1). However, there are other modes in FE analysis that our MD simulation did not show them. The reason can be related to the excitation zone and directions on the center of the beam (see Fig. 1). According to Fig. 4, the displacements changes at this nanobeams section in modes 4,5, and 7 has zero value, so the MD simulation did not detect them.

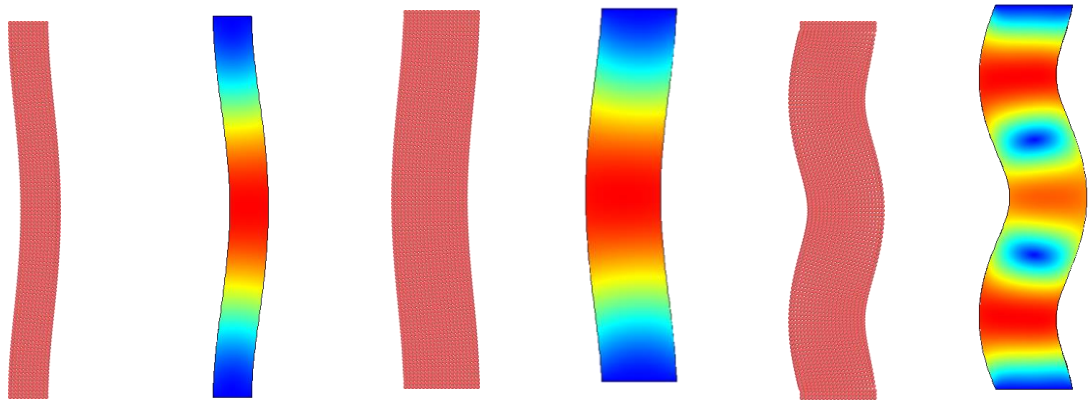

MD 1 FEM 1 MD 2 FEM 2 MD 3 FEM 9

Figure 5. The mode shapes from MD simulation and their counterparts from FEM simulations.

Table 1. Comparison of natural frequency values obtained from FE and MD methods.

	MD (GHz)	FEM (GHz)	Error (%)
(1,1)	18.165	18.168	0.0165
(2,2)	28.19	31.06	9.24
(3,9)	113.57	118.8	4.40

Fig. 6 compares the frequencies of nanobeams obtained from MD and FE methods vs. the crack depth and location. The general trend is to decrease the frequencies in all diagrams. Figures 6.a and 6.b also have more inconsistencies between the graphs. In the second and third modes, molecular dynamics simulations show a more significant percentage reduction in frequency values than the finite element simulation model (Figure 6.c -6.f).

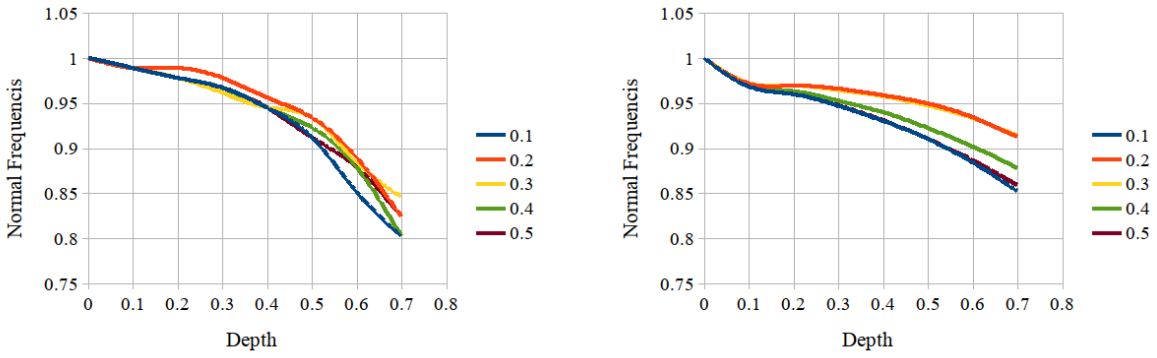

(a) (b)

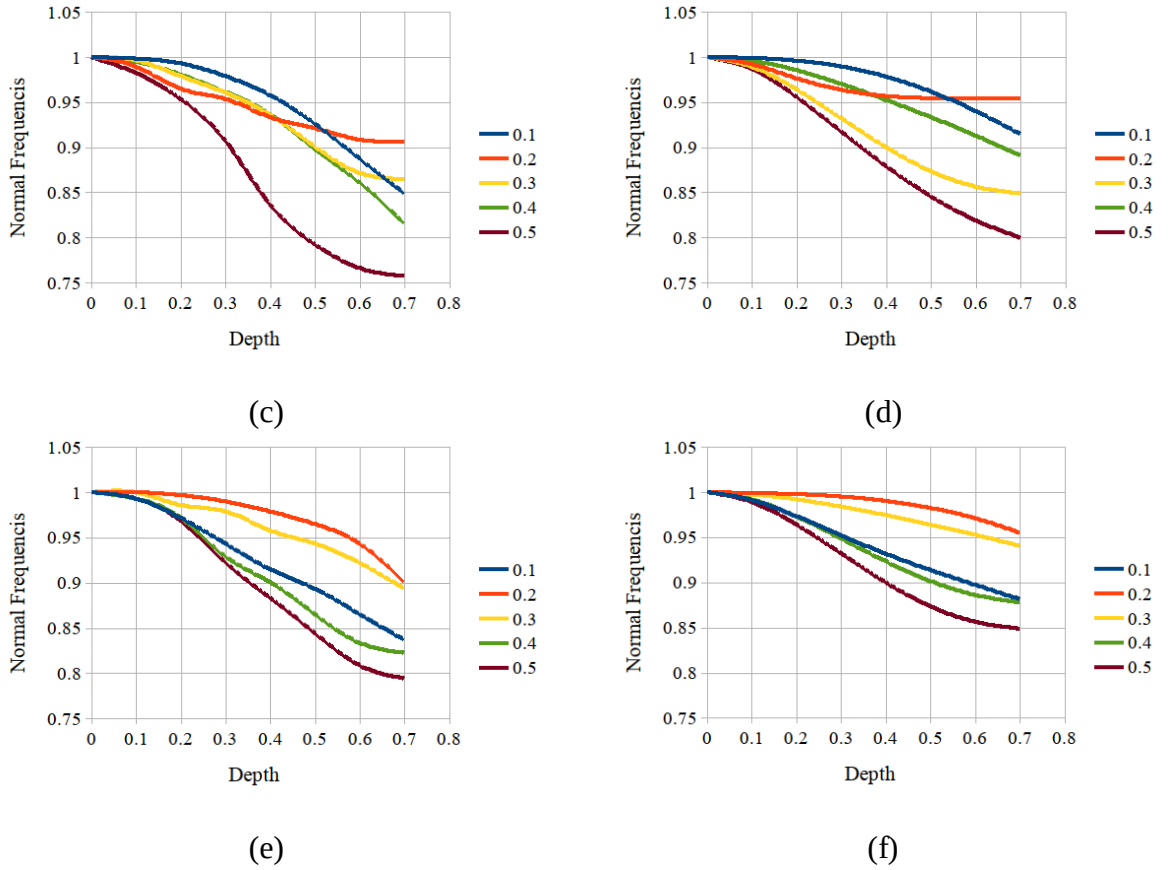

Figure 6. Compare cracked beam frequencies value between FEM and MD. **a:** mode 1 from MD **b:** mode 1 from FEM. **c:** mode 2 From MD **d:** mode 2 from FEM. **e:** mode 3 from MD and **f:** mode 9 from FEM

Figure 6. approve that the Finite element method data agreed with Molecular dynamics simulations. The slope of the graph at normalized depth equal to 0.1 in the first mode has changed (Figure 6. a-b). This change in the Finite element diagram is very clear, but molecular dynamic diagrams just show in crack position 0.2. there are some differences in the graphs, such as the ordering of decrease percent in the same depth. The finite element shows in a constant normalized depth, the crack at positions 0.1 and 0.5 have maximum effects in reducing frequencies, also crack at positions 0.2 and 0.3 has the same effects on the first natural frequencies. At the same time, the molecular dynamics graph can't be ordering effects of crack position on frequencies. The molecular dynamics show a larger reduction in natural frequencies. At the crack depth of 0.7, a larger percent reduction is occurring. The first mode shows a 20% and 16% reduction for the crack depth of 0.7 for the MD and FEM, respectively.

The second mode (Figure 6. c-d) shows maximum effects on frequencies is from the crack position of 0.5. there is about 25% and 20% reduction at the depth 0.7 for FEM and MD, respectively. Also, for crack position 0.2, there is the domain, from depth 0.3 to 0.7, that reduction in frequencies are uniform.

The third mode shows that the reduction in frequencies can be ordered based on crack positions—maximum and minimum reduction in a constant depth occur at crack positions 0.5 and 0.2, respectively. also, in all depth domain, the third natural frequencies reduction ordered by 0.5 > 0.4> 0.1 > 0.3 > 0.2 of cracks positions (Figure 6. e-f).

The second and third modes will be studied and compared with spring models in Timoshenko beam theory.

Crack models

From Timoshenko beam theory (1D), we have two sets of frequencies values; the first values are from the XZ plane and the other values from the YZ plane. The XZ plane values are related to MD 1 mode shape frequencies and YZ plane values, associated with MD 2 and MD 3 modes frequencies. In the following, the main criteria for naming will be the molecular dynamics simulation modes.

Figure 7 represent the dimensionless frequencies in the first and third mode of nanobeam. Model I and II (translational and rotational spring) have similar behavior in all domains (Fig 7). In mode 2, there are three extremum points in the position of crack 0.1, 0.23, and 0.5 that repeated in all models. For Mode 3, the extremum points occur in 0.2, 0.32, and 0.5 positions of beam length.

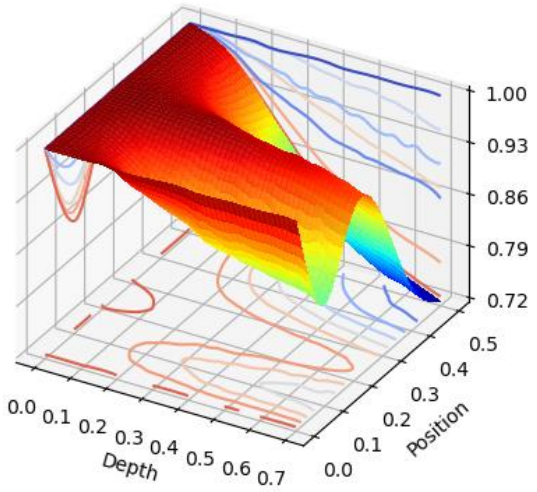

a1

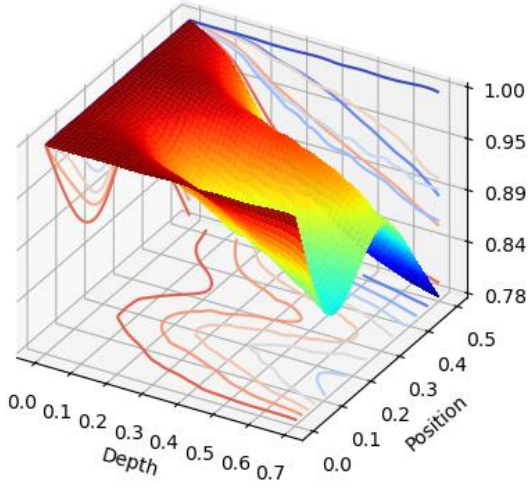

a2

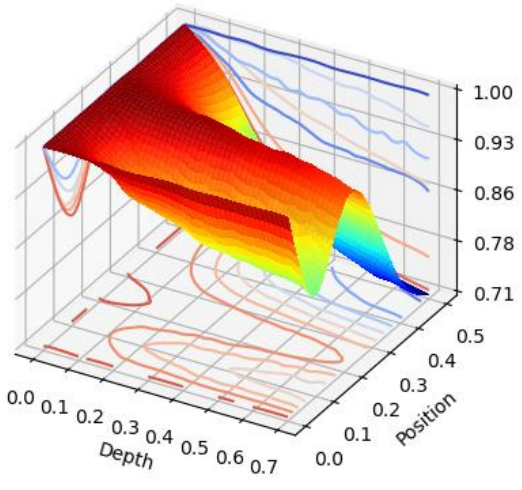

b1

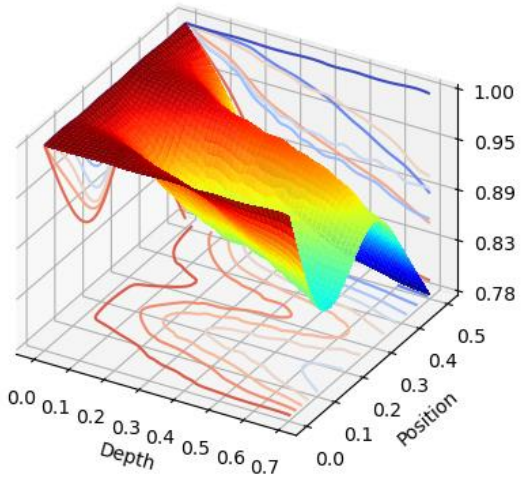

b2

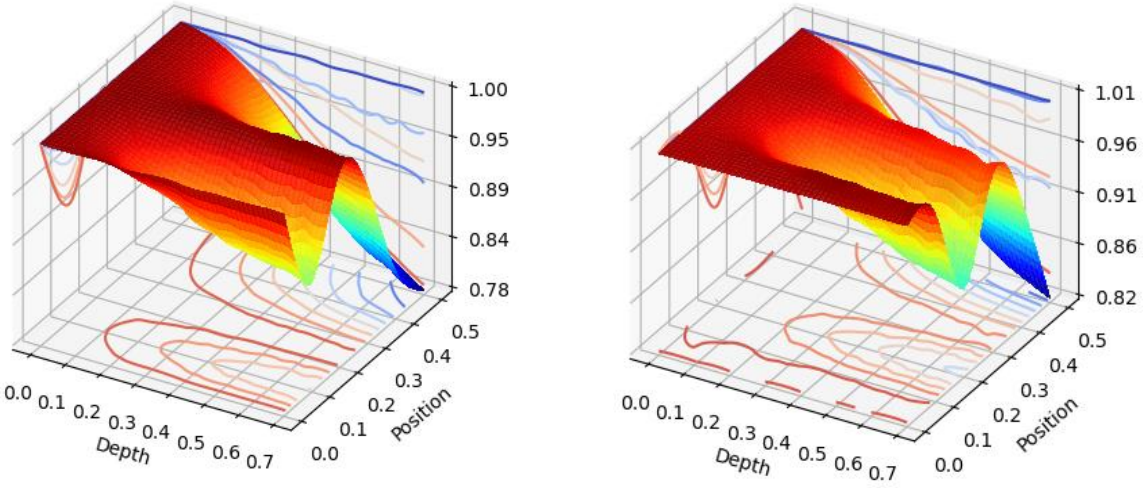

c1 c2

Figure 7. The mode graphs from (1D) models: model I **a1:** mode 2 a2: mode 3, model II **b1:** mode 2 **b2:** mode 3, model III **c1:** mode 2 **c2:** mode 3

In Model III, the value of frequencies in position 0.23 (Mode 2) and 0.32 (Mode 3) does not change, and they are equal to non-cracked of their values. For MODE I and Model I, the maximum, minimum, and Average error between Timoshenko theory and Molecular Dynamics results are 13.9 %, 0.13, and 4.22%, respectively. The most significant error occurs in the position equal to 0.5 and depth similar to 0.7. In the MODE I and Model III, in all domains, error occurs.

For MODE III, MD results have more similarity to Model I and II over than Model III. In Model III, by increasing crack depth, in position 0.32, the frequency value is constant, which caused the larger average error compared to Model I and II.

Figure 8 shows a comparison of frequency values for the methods used in this paper. As can be seen for the second mode, all theoretical models' behavior is consistent with each other. For the crack position at 0.3, the frequency value shows the most considerable reduction value at this crack position. In contrast, in the finite element and molecular dynamics models, the maximum decrease in the frequency value occurs when the crack is in 0.5 places. Also can see, That Models II and III have an agreement trend with Molecular dynamics and Finite element.

Of course, for the third mode, the order of decreasing the value of frequency in all models is consistent with the molecular dynamics model, and the farther the leaving position is from the boundaries and closer to the center of the beam, the more significant the decrease in the amount of frequency.

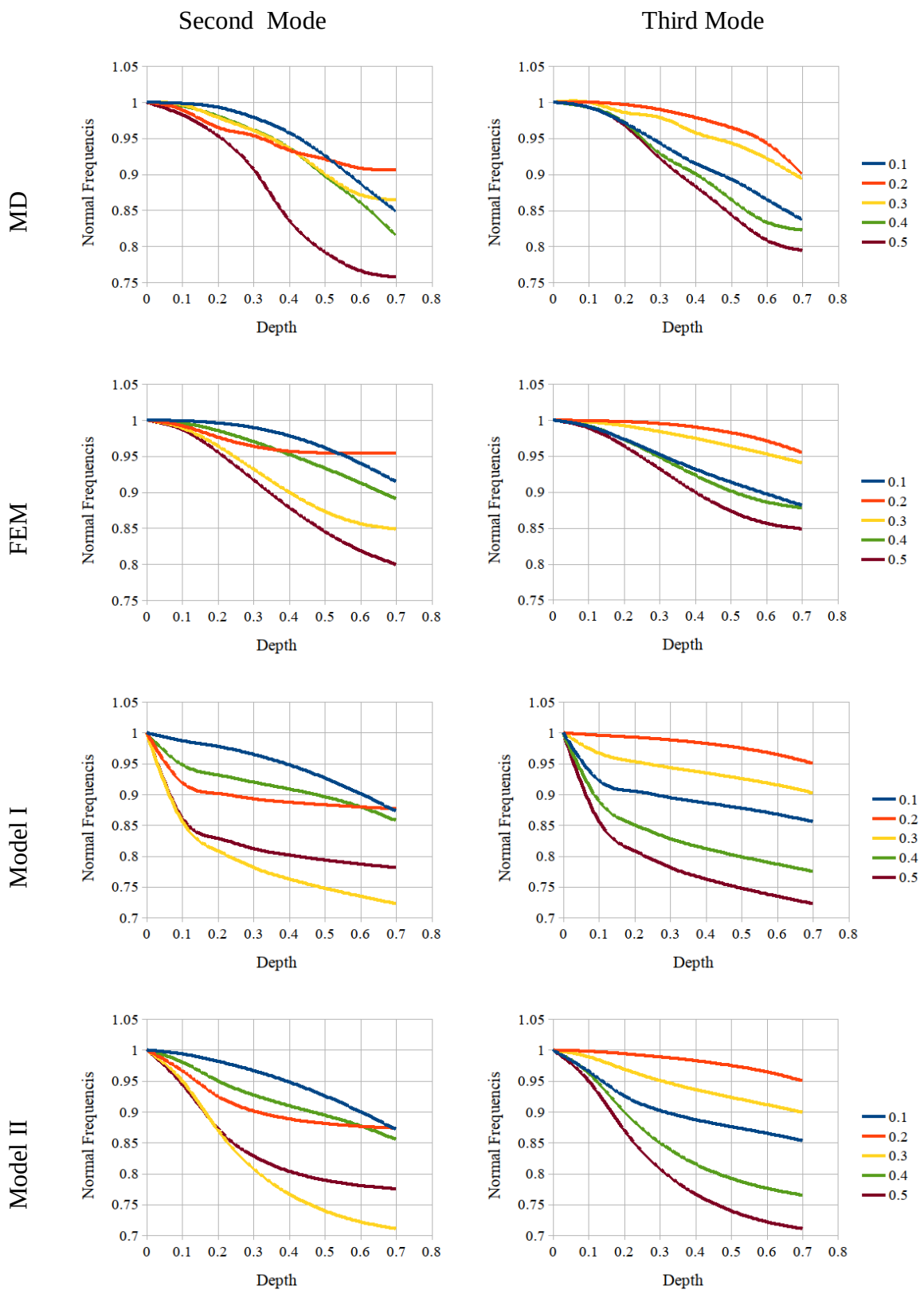
Second Mode
Third Mode
MD
FEM
Model I
Model II
Normal Frequencis
Depth
0.1
0.2
0.3
0.4
0.5

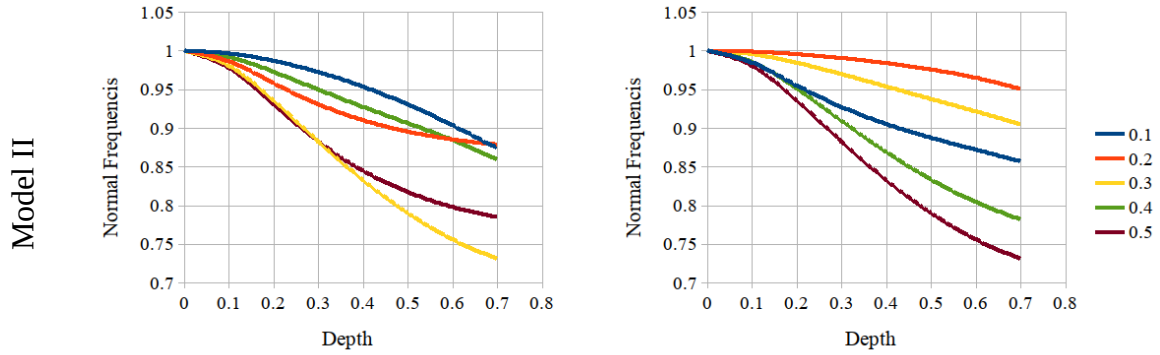

Figure 8. Comparison frequencies value for crack nanobeam

Conclusions

In the present study, Fe cracked nanobeams' vibrational behavior with a BCC structure was investigated by the Molecular Dynamics method, Finite Element, and the multiple models of the crack in Timoshenko beam theory. The effects of crack position and depth were scrutinized. The following observations and results were obtained:

1. the exiting zone and how the initial exiting nanobeam is important for detection mode shapes in molecular dynamics simulations.
2. The 3d Finite element method results agreed with the molecular dynamics data.
3. From MD and FEM results, the crack in the middle of the nanobeam has maximum effects on the value of natural frequencies.
4. Spring models show that in the second mode, the biggest reduction occurs when cracks are in 0.3 lengths of nanobeam. These results disagree with MD and FEM data.
5. When the crack is at the position of 0.2 lengths, in-depth range between 0.2 and 0.7, by increasing the depth, reduction of the second frequency in FEM and MD don't change, and it is constant at 5%, and 7% of nan cracked natural frequency of FEM and MD results, respectively.

References

[1] Husain, A., Hone, J., Postma, H. W. C., Huang, X. M. H., Drake, T., Barbic, M., ... & Roukes, M. L. (2003). Nanowire-based very-high-frequency electromechanical resonator. *Applied Physics Letters*, *83*(6), 1240-1242.

[2] Li, M., Mayer, T. S., Sioss, J. A., Keating, C. D., & Bhiladvala, R. B. (2007). Template-grown metal nanowires as resonators: performance and characterization of dissipative and elastic properties. *Nano letters*, *7*(11), 3281-3284.

[3] Liao, M., Hishita, S., Watanabe, E., Koizumi, S., & Koide, Y. (2010). Suspended Single-Crystal Diamond Nanowires for High-Performance Nanoelectromechanical Switches. *Advanced Materials*, *22*(47), 5393-5397.

[4] Wang, Z. L., & Song, J. (2006). Piezoelectric nanogenerators based on zinc oxide nanowire arrays. *Science*, *312*(5771), 242-246.

[5] P. Xie, Q. Xiong, Y. Fang, Q. Qing and C. M. Lieber, Nat. Nanotechnol., 2011, 7, 119-125.

[6] Eom, K., Park, H. S., Yoon, D. S., & Kwon, T. (2011). Nanomechanical resonators and their applications in biological/chemical detection: Nanomechanics principles. *Physics Reports*, *503*(4-5), 115-163.

[7] Kim, S. Y., & Park, H. S. (2008). Utilizing mechanical strain to mitigate the intrinsic loss mechanisms in oscillating metal nanowires. *Physical review letters*, *101*(21), 215502.

[8] Pourkermani, A. G., Azizi, B., & Pishkenari, H. N. (2020). Vibrational analysis of Ag, Cu and Ni nanobeams using a hybrid continuum-atomistic model. *International Journal of Mechanical Sciences*, *165*, 105208.
[9] Kowalczyk-Gajewska, K., & Maździarz, M. (2018). Atomistic and mean-field estimates of effective stiffness tensor of nanocrystalline copper. *International Journal of Engineering Science*, *129*, 47-62.
[10] Yang, X., Sun, Y., Wang, F., & Zhao, J. (2015). Surface effects on the initial dislocation of Ag nanowires. *Computational Materials Science*, *106*, 23-28.
[11] Ahadi, A., & Melin, S. (2016). Size dependence of the Poisson's ratio in single-crystal fcc copper nanobeams. *Computational Materials Science*, *111*, 322-327.
[12] Pishkenari, H. N., Afsharmanesh, B., & Akbari, E. (2015). Surface elasticity and size effect on the vibrational behavior of silicon nanoresonators. *Current Applied Physics*, *15*(11), 1389-1396.
[13] Reddy, J., Nonlocal theories for bending, buckling and vibration of beams. International Journal of Engineering Science, 2007. 45(2-8): p. 288-307.
[14] Wang, C. M., Zhang, Y. Y., & He, X. Q. (2007). Vibration of nonlocal Timoshenko beams. *Nanotechnology*, *18*(10), 105401.
[15] Behera, L. and S. Chakraverty, Free vibration of Euler and Timoshenko nanobeams using boundary characteristic orthogonal polynomials. Applied Nanoscience, 2014. 4(3): p.347-358.
[16] Wu, L.-Y., et al., Vibrations of nonlocal Timoshenko beams using orthogonal collocation method. Procedia Engineering, 2011. 14: p. 2394-2402.
[17] Eltaher, M., A. E. Alshorbagy, and F. Mahmoud, Vibration analysis of Euler–Bernoulli nanobeams by using finite element method. Applied Mathematical Modelling, 2013. 37(7): p.4787-4797.
[18] Beni, Y. T., A. Jafaria, and H. Razavi, Size effect on free transverse vibration of cracked nano-beams using couple stress theory. International Journal of EngineeringTransactions B: Applications, 2014. 28(2): p. 296-304.
[19] Hasheminejad, S. M., et al., Free transverse vibrations of cracked nanobeams with surface effects. Thin Solid Films, 2011. 519(8): p. 2477-2482.
[20] Loghmani, M. and M. R. Hairi Yazdi, An analytical method for free vibration of multi cracked and stepped nonlocal nanobeams based on wave approach. Results in Physics, 2018. 11: p. 166-181.
[21] Roostai, H. and M. Haghpanahi, Vibration of nanobeams of different boundary conditions with multiple cracks based on nonlocal elasticity theory. Applied Mathematical Modelling, 2014. 38(3): p. 1159-1169.
[22] Chondros, T. G., Dimarogonas, A. D., & Yao, J. (1998). A continuous cracked beam vibration theory. *Journal of sound and vibration*, *215*(1), 17-34.
[23] Barad, K. H., Sharma, D. S., & Vyas, V. (2013). Crack detection in cantilever beam by frequency based method. *procedia engineering*, *51*, 770-775.
[24] Mousavi Nejad Souq, S. S., & Baradaran, G. H. (2015). Crack detection in frame Structures with regard to changes in natural frequencies by using finite element method and ACOR. *Modares Mechanical Engineering*, *15*(8), 51-58.(in Persian)
[25] Khalkar, V., & Ramachandran, S. (2017). Vibration analysis of a cantilever beam for oblique cracks. *ARPN J. Eng. Appl. Sci.*, *12*(4), 1144-1151.
[26] Swamidas, A. S. J., Yang, X., & Seshadri, R. (2004). Identification of cracking in beam structures using Timoshenko and Euler formulations. *Journal of Engineering Mechanics*, *130*(11), 1297-1308.
[27] Khaji, N., Shafiei, M., & Jalalpour, M. (2009). Closed-form solutions for crack detection problem of Timoshenko beams with various boundary conditions. *International Journal of Mechanical Sciences*, *51*(9-10), 667-681.
[28] Batihan, A. Ç., & Kadioğlu, F. S. (2016). Vibration analysis of a cracked beam on an elastic foundation. *International Journal of Structural Stability and Dynamics*, *16*(05), 1550006.
[29] Viola, E., Nobile, L., & Federici, L. (2002). Formulation of cracked beam element for structural analysis. *Journal of engineering mechanics*, 128(2), 220-230.
[30] Yokoyama, T., & Chen, M. C. (1998). Vibration analysis of edge-cracked beams using a line-spring model. *Engineering Fracture Mechanics*, 59(3), 403-409.
[31] Mendelev, M. I., Han, S., Srolovitz, D. J., Ackland, G. J., Sun, D. Y., & Asta, M. (2003). Development of new interatomic potentials appropriate for crystalline and liquid iron. *Philosophical magazine*, *83*(35), 3977-3994.
[32] Plimpton, S. (1995). Fast parallel algorithms for short-range molecular dynamics. *Journal of computational physics*, *117*(1), 1-19.
[33] Loya, J. A., Rubio, L., & Fernández-Sáez, J. (2006). Natural frequencies for bending vibrations of Timoshenko cracked beams. *Journal of Sound and Vibration*, *290*(3-5), 640-653.
[34] Biswal, A. R., Roy, T., Behera, R. K., Pradhan, S. K., & Parida, P. K. (2016). Finite element based vibration analysis of a nonprismatic Timoshenko beam with transverse open crack. *Procedia Engineering*, 144, 226-233.

[35] Nguyen, K. V. (2014). Mode shapes analysis of a cracked beam and its application for crack detection. Journal of Sound and Vibration, 333(3), 848-872.
[36] Orhan, S. (2007). Analysis of free and forced vibration of a cracked cantilever beam. *Ndt & E International*, *40*(6), 443-450.
[37] Zeng, J., Ma, H., Zhang, W., & Wen, B. (2017). Dynamic characteristic analysis of cracked cantilever beams under different crack types. *Engineering Failure Analysis*, *74*, 80-94.
[38] Zheng, D. Y., & Kessissoglou, N. J. (2004). Free vibration analysis of a cracked beam by finite element method. *Journal of Sound and vibration*, *273*(3), 457-475.
[39] Ebrahimi, A., Meghdari, A., Behzad, M. (2005). A New Approach for Vibration Analysis of a Cracked Beam. International Journal of Engineering, 18(4), 319-330.
[40] Stukowski, A. (2009). Visualization and analysis of atomistic simulation data with OVITO–the Open Visualization Tool. *Modelling and Simulation in Materials Science and Engineering*, *18*(1), 015012.
[41] Shi, D., Wang, Q., Shi, X., & Pang, F. (2015). An accurate solution method for the vibration analysis of Timoshenko beams with general elastic supports. *Proceedings of the Institution of Mechanical Engineers, Part C: Journal of Mechanical Engineering Science*, *229*(13), 2327-2340.
[42] Tada, H., Paris, P. C., & Irwin, G. R. (1973). The stress analysis of cracks. Handbook, *Del Research Corporation*, 34.
[43] Lellep, J. A. A. N., & Lenbaum, A. R. T. U. R. (2016). Natural vibrations of a nano-beam with cracks. International Journal of Theoretical and Applied Mechanics, 1(1), 247-252.
[44] COMSOL, A. (2018). Comsol multiphysics® v. 5.4 www. comsol. com. Stockholm, Sweden. *COMSOL AB*.